The Submillimeter Extragalactic Background and its implication for the star formation history of the Universe

Guilaine Lagache, Jean-Loup Puget and Richard Gispert†
IAS, bât 121, Université de Paris XI, 91405 ORSAY Cedex

August 13, 1999

Abstract. The recently discovered Submillimeter Extragalactic Background (submm EB) has opened new perspectives on our understanding of galaxy evolution. We detail in this paper one of the major cosmological consequences of this discovery, the submm luminosity density history of the Universe.

Keywords: observational submillimeter cosmology

1. The Extragalactic Background (EB)

Our knowledge of the early epochs of galaxies has recently increased thanks to the observational evidence provided by UV/Vis/Near-IR, far-IR and submm surveys of high-redshift objects. In a consistent picture, the epoch of galaxy formation can also be observed by its imprint on the background radiation which is produced by the line-of-sight accumulation of all extragalactic sources.
The search for the UV, optical, near-IR and mid-IR EB (from 2000 $\AA$ to 15 μm) obtained by summing up the contributions of galaxies using number counts currently gives only lower limits. However, in the optical and near-IR the flatening of the faint counts obtained in the Hubble Deep Field suggests that we are now close to convergence. Thus we already have a good determination of the background in the optical and near-IR.
At longer wavelengths (λ >100 μm), a submm EB was predicted to exist as early as the 1970s. It has been detected for the first time only in 1996 by Puget et al. thanks to COBE data. Its detection, now confirmed by several other studies (Fixsen et al. 1998; Hauser et al. 1998; Lagache et al. 1999) has provided new perspectives for understanding galaxy evolution. The amount of energy in the submm EB is rather large. It exceeds the predictions based on extrapolations of the starburst galaxies as seen in the IRAS deep surveys by about a factor of 3 (Franceschini et al. 1994). Thus, it requires other sources, for example, spheroidal systems radiating mostly in the far-IR during their early evolution, or a high formation rate of massive stars at the early stages in the evolution of elliptical galaxies. Whatever the nature of the emitting sources, the background implies a very strong cosmological

evolution from the local galaxies to the more distant ones (Guiderdoni et al. 1998; Franceschini et al. 1998), with an enhancement of the IR emission at early stages of the galaxy evolution. This very strong evolution is also supported by the comparaison between the energy contained in the optical and submm EB. The sumtotal of the fluxes of the EB from 6 to 1000 μm is about 3.3 10^{-8} W m^{-2} sr^{-1} compared to 2 10^{-8} W m^{-2} sr^{-1} between the UV band and 6 μm. For the local galaxies, the energy ratio between IR and optical wavelengths is much smaller than that measured from the background (about 0.4 compared to 1.6). This simply reflects a strong change of galaxy properties between the local Universe and the more distant Universe. This change must affect the Star Formation (SF) history derived only from optical and near-IR observations of high-redshift objects. A significant fraction of SF might be hidden in heavily extinguished galaxies. These galaxies can be totally missed by optical surveys.

2. Star formation history

The history of the cosmic Star Formation Rate (SFR) can be derived from deep optical surveys assuming that (1) the stellar Initial Mass function is universal, (2) the far-UV light is proportionnal to the SFR and (3) extinction is negligible. The presence of dust which absorbes the UV starlight makes this last assumption not valid. The corrections needed to account for the extinction are rather uncertain and there is much controversy about the value of this correction. Moreover, the SFR deduced from optical surveys can be underestimated if there is a significant population of objects so obscured that they are not detected in these surveys. A way to avoid this dust contamination is to derive the SFR from the IR/submm surveys. However, so far, the catalogues of faint submm sources with reliable redshifts are not large enough to reconstruct the history of the SFR. But strong constraints can be provided by the inversion of the submm EB.

2.1. Inversion of the submm EB

For a Universe following the Robertson-Walker metric, the intensity of the submm EB (I_ν) can be simply related to the number of sources per Mpc^3 (N_z) having a luminosity L_{ν_0} using the expression:

$$\nu I_\nu = \frac{c}{4\pi} \int_{z=0}^{\infty} \int_{\nu_0=\nu}^{\infty} N_z L_{\nu_0} \frac{dt}{dz} d\nu_0 \quad \delta(\nu_0 - \frac{\nu}{1+z}) dz \qquad (1)$$

Choosing a spectral energy distribution L_{ν_0} and a cosmological model (i.e dt/dz), the inversion of Eq. 1 will give N_z. The variation of the

luminosity density as a function of redshift $\varphi(z)$, is then derived as follows:

$$\varphi(z) = N_z \int_{\nu_0} L_{\nu_0} d\nu_0 \quad L_\odot/Mpc^3 \tag{2}$$

Using such a formalism, the production rate of the far-infrared radiation as a function of redshift can be deduced using only one assumption: the spectrum of the galaxy L_{ν_0}. Since the submm EB seems to be dominated by luminous IR galaxies, as indicated by the ISO (Aussel, 1998) and SCUBA (e.g. Lilly et al. 1999) results, we choose a spectral energy distribution L_{ν_0} typical of starburst galaxies (Maffei, 1994; Guiderdoni et al. 1998). To determine $\varphi(z)$ (Eq. 2), we choose to explore the cases given by the combinations of: (1) three infrared galaxy luminosities: 3 10^{12} $L_\odot$, 5 10^{11} $L_\odot$ and 3 10^{10} $L_\odot$ (2) two values for the dust spectral index (-1.7 and -2) and (3) three cosmological models defined by the set of parameters h, Ω_0 and Ω_Λ (h=0.65, Ω_0=0.3, Ω_Λ=0.7; h=0.65, Ω_0=0.3, Ω_Λ=0, and h=0.65 Ω_0=1, Ω_Λ=0) which fixes the dt/dz. The basic algorithm for finding N_z is based on Monte Carlo simulations. N_z is sampled at a few redshift values and linearly interpolated between these values for computing the term on the right of Eq. 1. It has been assumed that beyond z=13, N_z=0. The best evaluation (minimum χ^2) has been obtained by exploring a wide range of randomly distributed values of N_z. Error bars are estimated by keeping the computed submm EB (1) within the submm EB uncertainties at each sampled frequency and (2) greater than the lower submm EB limit at 850 μm from Barger et al. (1999). By using an iterative method for progressively reducing the range of explored values, we reach convergence for each case studied with a reasonable number of hits ($\sim$ 50000). For the submm EB (I_ν in Eq. 1), we use the FIRAS and the DIRBE 140 and 240 μm determinations of Lagache et al. (1999). $\varphi(z)$ at z=0 has been fixed following Soifer & Neugeubauer (1991): for h=0.65, we have $\varphi(z=0)$=1.07 10^8 $L_\odot$/Mpc^3.

2.2. Main result

Results for $\varphi(z)$ are presented in Fig. 1a for a fixed cosmological model and three different luminosities. We note that the combination of all parameter sets gives results consistent within a factor of two. As was expected, constraints on $\varphi(z)$ are very weak below redshift 1 (no EB values below 140 μm) and above 4 (very low signal to noise ratio of the FIRAS submm EB above 800 μm). Between redshifts 1.5 and 3.5, the submm EB gives strong constraints. The luminosity density is about 10 times higher at z=1.4 than at z=0 and it is nearly constant up to

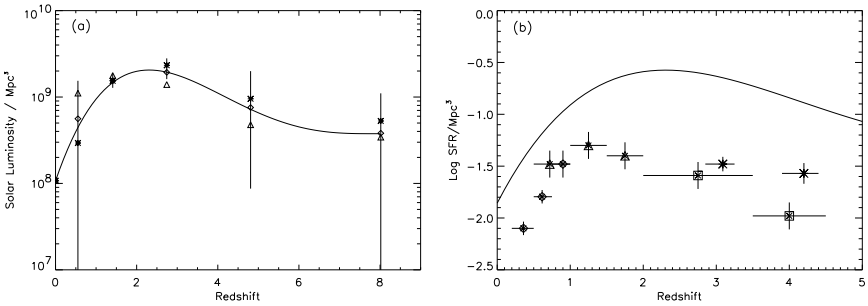

Figure 1. (a) Luminosity density distribution as derived from the submm EB for a given cosmological model (h=0.65, Ω_0=0.3, Ω_Λ=0.7) and dust spectral index ($\alpha = 2$) with three different luminosities (stars: 3 10^{12} $L_\odot$, diamonds: 5 10^{11} $L_\odot$, triangles: 3 10^{10} $L_\odot$). The error bars represent the uncertainties derived for the star points. Also represented is the analytical function that reproduces the case L=5 10^{11} $L_\odot$, Ω_0=1 and Ω_Λ=0. The analytical function is $10^{az^3+bz^2+cz+d}$ with a=-2.42 10^{-3}, b=5.78 10^{-2}, c=1.36 and d=8.03. (b) SFR derived from the submm EB (analytical function, continuous line) and UV/Vis/Near-IR observations (diamonds: Lilly et al. 1996; triangles: Conolly et al. 1997; squares: Madau et al. 1996 and crosses: Steidel et al. 1999)

redshift 4. Data points derived from optical observations (Fig. 1b)[1] are lower by a factor of about 5 than our determination. This clearly shows that the optically-derived SFR is severely underestimated due to the presence of dust.

References

Aussel, H., 1998, PhD thesis.
Barger, A.J. et al. *ApJ*, 518:L5, 1999.
Connolly, A.J. et al. *ApJ*, 486:L11, 1997.
Fixsen, D.J. et al. *ApJ*, 508:123, 1998.
Franceschini, A. et al. *MNRAS*, 296:709, 1998.
Franceschini, A. et al. *ApJ*, 427:140, 1994.
Guiderdoni, B et al. *MNRAS*, 295:877 , 1998.
Hauser, M.G. et al. *ApJ*, 508:25, 1998.
Lagache, G. et al. *A&A*, 344:155, 1999.
Lilly, S.J. et al. *ApJ*, 518:641, 1999.
Lilly, S.J. et al. *ApJ*, 460:L1, 1996.
Madau, P. et al. *MNRAS*, 283:1388, 1996.
Maffei, B. *PhD Thesis*, Paris XI University, 1994.
Puget, J.L. et al. *A&A*, 308:L5, 1996.
Soifer, B.T. & Neugebauer, G. *ApJ*, 101:354, 1991.
Steidel, C.T. et al., *ApJ*, in press, 1999.

[1] To compare the star formation rate with the luminosity density, we use: $\frac{SFR}{M_\odot yr^{-1}} = \frac{L_{IR}}{7.710^9 \quad L_\odot}$ (Guiderdoni et al. 1998)